Influence of the Nb/P ratio of acidic Nb-P-Si oxides on surface and catalytic properties

A. Gervasini,[a,b,*] S. Campisi,[a] P. Carniti,[a,b] M. Fantauzzi,[c,d] C. Imparato,[f] N. J. Clayden,[e] A. Aronne,[f,*] A. Rossi[c,d]

[a] *Dipartimento di Chimica, Università degli Studi di Milano, via Camillo Golgi, 19, I-20133 Milano, Italy*

[b] *CNR-Istituto di Scienze e Tecnologie Molecolari, via Camillo Golgi 19, I-20133 Milano, Italy*

[c] *Dipartimento di Scienze Chimiche e Geologiche, Università degli Studi di Cagliari, Campus di Monserrato S.S. 554, Italy*.

[d] *INSTM, UdR, Cagliari, Italy*

[e] *School of Chemistry, University of East Anglia, Norwich NR4 7TJ, United Kingdom (UK).*

[f] *Dipartimento di Ingegneria Chimica, dei Materiali e della Produzione Industriale, Università degli Studi di Napoli Federico II, P.le Tecchio 80, 80125 Napoli, Italy*.

* Corresponding author(s). A. Gervasini, Università degli Studi di Milano and A. Aronne, Università degli Studi di Napoli Federico II

ABSTRACT

In this work, two acidic Nb-P-Si mixed oxide gel-derived materials characterized by Nb/P molar ratios equal to 2 (5Nb2.5P) and 1 (2.5NbP) were investigated for their surface and bulk properties in relation with the catalytic performances in the fructose dehydration reaction.

The structural characteristics of the studied samples and the changes occurring after water treatment and after reaction were investigated by ^{29}Si and ^{31}P solid state nuclear magnetic resonance (MAS-NMR) and X-ray photoelectron (XPS) spectroscopies, while the characterization of their acidic properties was performed by base (2-phenylethylamine) adsorption in liquid phase.

MAS-NMR showed that the phosphorus remains firmly anchored into the siloxane matrix after exposure to cold water for 5Nb2.5P sample and XPS confirmed the homogeneity of the sample composition. Both samples exhibited good *intrinsic* acidity and maintained significant *effective* acidity in polar-protic liquids; 2.5NbP manifested a double amount of acid sites compared to 5Nb2.5P, when 2-phenylethylamine is used as probe.

Fructose dehydration to 5-(hydroxymethyl)furfural (HMF) on the two gel-derived catalysts was performed in water and in water-isopropanol solution under mild conditions (130°C) working in a recirculation reaction line comprising a tubular catalytic reactor. In water-isopropanol solution, the samples displayed good performances, as expected thanks to the lively *effective* acidity. Around 45-50% fructose conversion was attained on both samples, with selectivity to HMF equal to about 50% on 2.5NbP gel-derived catalyst. Recycling tests showed satisfactorily stable activity during three consecutive runs.

***Keywords*:**

Nb-P-Si mixed oxides; solid acid catalyst; effective acidity; fructose dehydration; biomass valorization; 5-hydroxymethyl-2-furaldehyde (HMF), XPS, MAS-NMR.

1. Introduction

The feasibility to establish a more sustainable economy and carbon-neutral society is related to the improvement of the efficiency of biomass transformation to value-added chemicals, that in turn requires the development of new functionalized catalysts [1]. These new materials should be synthesized by environmentally friendly procedures and should exhibit suitable functionalities such as the stability in *benign solvents,* among them water, in order to realize sustainable biomass valorisation processes. In the case of acid catalysts, the tolerance to water becomes a trade-off between the strength of acid sites of the material and its reactivity towards water.

Recently, an innovative hydrolytic sol-gel route, distinguished by the easy manipulation of precursors and wholly performed at room temperature, was established by the authors, allowing to prepare amorphous Nb-P-Si mixed oxide materials, with a molar ratio Nb/P = 1 and SiO_2 content ranging from 95 to 80 mol % [2]. Si–O–Nb bridges allowed phosphorus to be stably anchored through Nb–O–P bonds within the gel. Moreover, a large amount of OH groups was retained in the structure of these solids even after heating at temperatures higher than 500 °C. These materials, presenting peculiar acidic properties with high concentration of both Brønsted (BAS) and Lewis (LAS) acid sites, were tested in the hydrolysis of inulin as well as in the esterification of oleic acid with polyalcohols, showing good catalytic performances [3-4]. Particularly, the solid with molar composition $2.5Nb_2O_5 \cdot 2.5P_2O_5 \cdot 95SiO_2$ (2.5NbP) showed for both studied reactions higher activity and better stability in the reaction medium than well-known niobium oxophosphate, considered one of the best water-tolerant acid catalysts. Indeed, for this catalyst the high concentration of BAS and LAS sites was for the most part preserved after treatment in water, especially concerning BAS sites. Only a partial removal of strong BAS occurred, associated with some loss of the less polymerized phosphorus Q_1' units [3]. Phosphorus leaching is actually the main drawback shown by any P-containing material in contact with water due to the strong chemical affinity between phosphorus and water.

In this work a new Nb-P-Si solid acid with $5Nb_2O_5 \cdot 2.5P_2O_5 \cdot 92.5SiO_2$ (5Nb2.5P) molar composition was designed aiming to the minimization of P leaching: considering the bridging role of Nb, it is expected that doubling its content would enhance the stability of phosphate units in water. The structural, morphological and surface acidic properties of this material were compared with the ones of 2.5NbP. Moreover, its catalytic performances were tested in a very important reaction of biomass valorisation: the dehydration of fructose to 5-hydroxymethyl-2-furaldehyde (HMF). HMF can be considered as one of the most promising building block compounds in biorefinery processes since it acts as a platform molecule bridging biomass chemistry and petrochemistry [5, 6].

The dehydration of fructose in acidic conditions involves a complex set of chemical reactions leading to intermediates, HMF, and several reaction by-products, such as levulinic and formic acids derived from the further rehydration of HMF when high Brønsted acidity is present on the catalyst. Moreover, formation of humins by polymerization reactions represents the most severe problem that limits the reaction application at industrial scale. Very high yields to HMF are obtained using aprotic organic solvent such as dimethyl sulfoxide, but the high boiling point of this solvent as well as its toxicity make largely unfavourable its use for large-scale biomass transformation. Therefore, heterogeneous catalysed reaction in liquid water represents a target to develop risk-free chemical processes that deeply respect the criteria of environmental sustainability.

Several papers in the literature have already reported about the good catalytic activity of Nb-containing catalysts in water in the dehydration reaction of fructose [7-9]. Unfortunately, in water the activity of the catalysts was rapidly lost and a decreasing exponential trend of fructose conversion against reaction time was observed [9]. The noticed loss of activity might be ascribed to the deposition of insoluble *humins* on the surface acid sites [7-8, 10-11].

With the intent to limit the problems occurring in water, in this work the fructose dehydration reaction has been investigated also in water-isopropanol mixture, which might be able to maintain in solution a higher amount of *humins* or by-products than water, so improving the catalyst stability.

Accordingly, the two catalysts derived from the 2.5NbP and 5Nb2.5P gels have been tested in water and in water-isopropanol solution. The influence of Nb-concentration and Nb/P ratio on surface properties and catalytic activity has been comparatively studied.

2. Experimental section

2.1. Materials

A niobium-phosphorus-silicon mixed oxide material with $5Nb_2O_5 \cdot 2.5P_2O_5 \cdot 92.5SiO_2$ (**5Nb2.5P**) nominal molar composition was prepared by a sol-gel procedure previously described [2] except for the Nb/P molar ratio that in this case was set equal to 2. In this procedure, completely performed at room temperature, phosphoryl chloride, $POCl_3$ (99%, Aldrich Chemical), niobium chloride, $NbCl_5$ (99%, Gelest), and tetraethoxysilane, $Si(OC_2H_5)_4$ (99%, Gelest, TEOS), and anhydrous ethanol (EtOH) were used as starting materials and solvent, respectively.

The different reactivity of the precursors was controlled and homogenised by dissolving them in EtOH, adjusting the pH and adopting a suitable mixing sequence [2]. The final solution, with molar ratios TEOS:H_2O:Nb:P = 1:4:0.054:0.027, was hydrolysed obtaining a transparent and homogeneous gel within a few days. The gel was fully dried in air at 110 °C in an electric oven for 3 days. Amorphous gel-derived catalyst was obtained by annealing the dried gel at 500 °C for 1 h with heating rate of 5°C min^{-1}, followed by quenching (5Nb2.5P-500).

For comparative purpose, a gel-derived sample with $2.5Nb_2O_5 \cdot 2.5P_2O_5 \cdot 95SiO_2$ (**2.5NbP**) nominal molar composition, characterized by the Nb/P molar ratio equal to 1, was also prepared by the same procedure (2.5NbP-500).

By analogy with the 2.5NbP sample to test the effective water tolerance of the 5Nb2.5P-500, it was treated in water under vigorous stirring for 16 h at room temperature (5Nb2.5P-500-w).

2.2 Characterization of dried gel and gel-derived catalysts

Specific surface area of the catalysts was computed by the Brunauer, Emmett and Teller (BET) and t-plot (by using the reference Harkins-Jura isotherm) methods; porosity was determined by N_2

adsorption/desorption isotherms collected at -196 °C using an automatic analyser of surface area (SA™ 3100 version instrument from Beckman Coulter). Pore size distribution (PSD) was computed by Barrett-Joyner-Halenda (BJH) model equation from the desorption branch of the collected isotherms. Prior to the analysis, fresh and thermally treated samples (0.05-0.1 g) have been outgassed at 150°C for 3 h under vacuum.

The determination of the acid sites of the two samples was carried out by using 2-phenylethylamine (PEA) as basic probe in cyclohexane (Sigma-Aldrich, > 99.5%) for the *intrinsic* acidity and in water (Sigma-Aldrich, HPLC grade) and in water-isopropanol (20% isopropanol, Sigma-Aldrich, 99.9%) liquid mixture for the *effective* acidity. Adsorption was carried out in an adsorption line comprising a HPLC and working in complete recirculation, specifically assembled for this purpose [12-13]. The samples (ca. 0.03-0.05 g) were placed in a sample holder (stainless steel tube, 2 mm i.d. and 12 cm length), mounted in place of the chromatographic HPLC column, and maintained at constant temperature (30.0±0.1°C) between two sand pillows. Prior to the measurement, the samples were activated at 150 °C overnight in flowing air (8 $mL \cdot min^{-1}$) and then filled with the liquid (cyclohexane or water or water-isopropanol). Successive dosed amounts of PEA solution (50 μL, ca. 0.10 M) were injected into the line in which the liquid continuously circulated, until adsorption equilibrium was achieved. From the step-chromatogram obtained, it was possible to construct the relevant isotherm of PEA adsorption on the acidic surface. The amount of acid sites was determined by modelling the collected adsorption curve with the Langmuir model equation; from the linearized equation the parameter representing the maximum amount of PEA adsorbed can be computed. By assuming a 1:1 stoichiometry for the PEA adsorption on the acid sites, the maximum amount of acid sites ($mequiv \cdot g^{-1}$) could be determined.

^{29}Si and ^{31}P NMR spectra were acquired by direct polarization (DP) magic angle spinning (MAS) technique with a Bruker AVANCE 300 (Bruker Biospin, Milan, Italy) magnet equipped with a 4 mm wide-bore MAS probe and operating at ^{29}Si and ^{31}P, resonating frequencies of 59.6 and 121.5 MHz, respectively. Samples were packed in 4 mm zirconia rotors with Kel-F caps and

spun at 10 000 ± 1 Hz. Each spectrum was processed using Bruker Topspin software (v.2.1). In particular, the free induction decays (FID) of ^{29}Si and ^{31}P spectra were Fourier transformed (FT) by applying 8 and 4 k zero filling and adopting an exponential filter function, with a line broadening of 100 and 50 Hz, respectively. Each spectrum was phase and baseline corrected.

XPS spectra were recorded on powdered samples pressed on copper bi-adhesive tape. The analyses were carried out using an ESCALAB MKII (Vacuum Generator Ltd, East Grinstead, UK) upgraded to five channelectrons. The X-ray source was Al $K\alpha_{1,2}$ ($h\nu$ = 1486.6 eV) operating at 20 mA and 15 kV (300 W). The base pressure was 10^{-7} Pa and the analyser was operated in constant analyser energy mode (CAE). Survey scan spectra were acquired at 50 keV pass energy while the pass energy for the narrow scan spectra was set at 20 keV. The energy scale was calibrated according to ISO 15472:2001 – surface chemical analysis – X-ray photoelectron spectrometers – calibration of energy scale. The full width at half maximum (FWHM) at the peak height of Ag $3d_{5/2}$ acquired under the same experimental conditions was 1.1 eV and the intensity/energy response function was evaluated to be equal to $KE^{-0.5}$. The uncertainty on the binding energy values was estimated to be equal to ± 0.2 eV while the accuracy of the quantitative analyses was found to be ±10% for the P signal.

2.3 Catalytic Activity

The tests of catalytic dehydration of fructose were performed in a total recirculation reaction line (Scheme S1) already employed in previous works [14-15]. The apparatus comprises: a HPLC pump (Merck-Hitachi L-6200), a stainless-steel pre-heater and fixed-bed flow reactor, both in stainless steel and put in a thermostatic oven, and a jacked reservoir for the feeding solution, maintained at 17°C. The fructose solution was continuously sent from the reservoir to the reactor and the solution exiting from the reactor was mixed in the reservoir with the remaining solution (under stirring). So, the solution continuously recirculated (3 $mL \cdot min^{-1}$) all along the reaction time. Based on kinetic consideration [14-15], if the flow rate was sufficiently high, the reaction data could be treated as if it would have been conducted in a conventional batch reactor. By this reaction set-up, it was easy to

make withdrawals of the solution at given intervals of time, avoiding problems associated with the presence of catalyst powder, filtration, and modification of contact time.

Before the use, the chosen catalysts were pressed, ground, sieved (20-45 mesh) and finally dried overnight at 120°C. A given quantity (ca. 0.5 g) of so prepared catalyst was put in a stainless steel tubular reactor, between two sand pillows and two swabs of stainless steel wool. Test carried out with the reactor only filled with sand and stainless steel wool showed the materials inertia under the reaction conditions. The reaction tests were carried out at 130°C in water or in liquid water-isopropanol (20%) solution, containing 0.1 M initial fructose concentration; the presence of needle valves allowed maintaining an overpressure that guaranteed the liquid phase, in any case. The reaction line can operate up to 10 bar of pressure in order to work in liquid-solid heterogeneous phase.

The progress of the reaction was checked by performing periodic withdrawals of 0.5 ml of solution directly from the reservoir. The first sample was taken 30 min after the beginning of the reaction. Each test was run until the attainment of ca. 50% fructose conversion. At the end of the first activity test performed on the fresh catalyst, the solution was removed and the entire line, including the catalyst, was washed in flow with the pure solvent for 1 h. The catalyst was made to work again by feeding a fresh 0.1 M fructose solution (second run activity). If good activity was maintained, three activity runs were carried out on the same catalyst.

The reaction products were analysed by a liquid chromatograph (HPLC) equipped with an injector (Waters U6K), a pump (Waters510), a column heater (Waters CHM) and a refractive index detector (Waters 410). The analyses were carried out with a Sugar-Pak 1 (Waters) column operating at 90°C and eluted with a solution of CaEDTA 10^{-4} M in water (0.5 $mL \cdot min^{-1}$). In the catalytic tests, both the unreacted fructose and the formed reaction products (glucose, HMF, soluble condensation products, some of them not yet completely identified) have been quantified and the concentrations were expressed in terms of monosaccharide equivalents. The results of the analyses could be

affected by an average standard error of about 5%. By comparing the initial and the final monosaccharide equivalents, the mass balance was always over 95% (Fig. S1).

3. Results and discussion

3.1. Solid state NMR

^{29}Si and ^{31}P solid state NMR spectra of 5Nb2.5P, 5Nb2.5P-500 and 5Nb2.5P-500-w are shown in Fig. 1. Different degrees of connectivity of the structural units making up the material give rise to distinct chemical shifts ranges in both the ^{29}Si and ^{31}P NMR spectra where the connectivity is described by the Q_N notation, with N the number of bridging oxygen of the tetrahedral unit. The relative proportions of these structural units were determined by fitting the experimental ^{29}Si and ^{31}P NMR lineshapes to a set of Gaussian functions using the program GFIT with non-linear least squares fitting based on the Levenberg-Marquardt method. Results of the curve fitting are shown in Tables 1 and 2 for the ^{29}Si and ^{31}P NMR spectra, respectively.

Cross-linking is shown by the Q_3 and Q_4 resonances while linear chain formation would be shown by the Q_2 resonance. All 5Nb2.5P samples gave ^{29}Si NMR spectra with a similar proportion of the various Q_N resonances, Table 1. Such differences, detected between the three samples, are minor and are probably a result of sample variability rather than being an indication of any effect caused by sample treatments. Consequently the siloxane network appears to be largely unaffected by the thermal treatment or exposure to water. Comparisons with the previously reported ^{29}Si NMR spectra obtained for the 2.5NbP sample are complicated by the much poorer signal-to noise ratio seen for the 2.5NbP material. Fitting to broad lineshapes can be uncertain in these cases, with local minima hindering the analysis. Indeed it is often necessary to start the fit with parameters close to what is thought to be the likely composition. Using such an approach with the 5Nb2.5P fits as a guide, the 2.5NbP dried gel ^{29}Si NMR data was re-evaluated and a fit closer to the current 5Nb2.5P dried gel data was obtained. This suggests that the previous analysis overemphasised the degree of

cross-linking in the siloxane matrix and indicates increasing the niobium content does not modify the siloxane matrix significantly. No direct evidence, for anchoring of the niobium into the siloxane matrix, in the nature of an additional Q_N(Nb) resonance, is to be expected at these niobium compositions given the broad nature of the lineshapes and the small effect niobium has been shown to have on the ^{29}Si chemical when forming an Si-O-Nb bond.

The 5Nb2.5P dried gel shows evidence for a small amount of isolated phosphate, otherwise all the intensity is in a chemical shift range identified as being consistent with an Nb-O-P (see Table 2). Owing to the variability in the chemical shift it is not possible to entirely rule out P-O-P, especially for the resonance at -7.4 ppm. Upon thermal treatment at 500°C a new set of resonances appear with one around -5.3 ppm still consistent with an Nb-O-P connectivity. For the other resonances, one at -12.0 and the other at -19.9 ppm the chemical shifts are consistent with a terminal phosphate or chain phosphate. But there remains the possibility the resonance at -12.0 ppm could be associated with niobium. Unfortunately the uncertainty in the nature of the connectivity, phosphorus or niobium to phosphorus, cannot be resolved in these amorphous materials because the more sophisticated NMR correlation experiments necessary are exceedingly difficult to perform. Despite this uncertainty the most significant feature is that exposure of the material to water, after being heat-treated (5Nb2.5P-500-w), had a negligible effect on the proportions of the different resonances seen. Consequently whatever the true assignment of these resonances their continued presence shows that the phosphorus remains firmly anchored into the siloxane matrix after exposure to cold water.

3.2. Morphological characteristics and acidity determination

The morphology of 2.5NbP-500 (Nb/P=1), characterized by the presence of both micropores and mesopores, has been already studied [3]; it is interesting to compare this sample with that obtained doubling the amount of Nb in the composition (5Nb2.5P-500 with Nb/P=2). The analysis of N_2

adsorption/desorption isotherms (Fig. 2), which allowed us to evaluate both the morphological features listed in Table 3 and the pore size distribution (PSD) plots displayed in Fig. S2, evidences the microporous nature of 5Nb2.5P-500 sample. In fact, it shows a negligible pores population with size larger than 2 nm and no hysteresis loop in its isotherm curves. For Nb-P-Si samples characterised by Nb/P = 1 a strong decrease of specific surface area was observed with the increasing of the Nb (P) content, associated with a variation of the porosimetric distribution [4]. These effects were related to the increase of cross-linking degree of Nb and P units, along with the decrease of SiO_2 mass content [4]. The different morphological properties between the 2.5NbP-500 and 5Nb2.5P-500 samples can be similarly due to a structural effect as a consequence of the role exerted by Nb as bridge between Si and P units and of the reduced amount of SiO_2 moving from 84.8 to 76.7 wt%.

The surface of the Nb-P-Si oxides is characterized by acid sites presence comprising both Brønsted acid sites (P-OH, Nb-OH, and Si-OH) and Lewis acid sites (tetrahedral Nb species). A thorough characterization of the acidity of 2.5NbP-500 has been presented in Ref. [3] with measurement of the acid sites performed in cyclohexane (*intrinsic* acidity) and in water (*effective* acidity). Also the Brønsted or Lewis nature of the acid sites was spectroscopically determined by pyridine adsorption under dry and wet conditions; the Lewis to Brønsted ratio moved from 1.06, determined under dry condition, to 0.39 under wet conditions, indicating that Brønsted sites population predominates in water.

The result obtained from the isothermal (30°C) measurements of PEA adsorption on the 5Nb2.5P-500 surface in cyclohexane (*intrinsic* acidity) can be compared with that on 2.5NbP-500 already presented [3]. Much lower amount of PEA adsorption was obtained on 5Nb2.5P-500 (Table 3), whose surface has around one third of acid sites with respect to 2.5NbP-500 surface. This unexpected result could be justified considering the remarkable morphological difference between the two samples. The almost absence of mesopores of the 5Nb2.5P-500 sample may lower the fraction of exposed and available acid sites. In fact, acidity titration by using ammonia gave similar

results for the two samples (*ca*. 0.7 mequiv·g^{-1}), suggesting that it is microporosity responsible of the limited acidity determined on 5Nb2.5P-500 by using PEA. This remark is also in agreement with the correlated catalytic results (see paragraph 3.4).

Acidity of the two calcined samples has also been determined in the two solvents used in the catalytic reaction (water and water-isopropanol) to collect information on the *effective* acidity of the two surfaces under real operative conditions. The PEA adsorption isotherms in water and in water-isopropanol solution for 2.5NbP-500 and 5Nb2.5P-500 surfaces are shown in Fig. 3, and the computed amount of acid sites (mequiv·g^{-1}) in the two liquids is reported in Table 3. The PEA adsorption isotherms were Langmuirian shaped, in any case, with the adsorption curves of 2.5NbP-500 laying over those of 5Nb2.5P-500. On the latter sample, the total amount of acid sites is about half than on 2.5NbP-500, both in water and in water-isopropanol solution. The higher amount of Si-O-Nb-O-P cross-links at the surface of 5Nb2.5P-500 may stabilise the NbO_6 and PO_4 units towards hydrolysis, therefore reducing the amount of Nb-OH and P-OH groups initially present on the surface.

As a matter of fact, comparing the *intrinsic* and *effective* acidities for the 5Nb2.5P-500 sample, it appears only a slight decrease of the amount of acid sites determined in water (ca. 10% lower) and in water-isopropanol solution (ca. 25% lower) with respect to those determined in cyclohexane. This indicates that the acid sites of 5Nb2.5P-500 are *water-tolerant* [16-18], with the main contribution of Brønsted sites associable with terminal or bridging phosphorous or niobium (X–OH and X–O(H)–Y with X, Y = P and Nb). A different behaviour appeared concerning the *intrinsic* and *effective* acidities of 2.5NbP-500, the acidity exhibited in water and in water-isopropanol solution was almost half of that in cyclohexane. In this case, the surface has also a high amount of very weakly acid sites, like Si-OH, that can be titrated only in the organic solvent and not in highly polar-protic liquids [12, 19].

3.3. XPS analysis

The 5Nb2.5P dried gel and 5Nb2.5P-500 were characterized by XPS, along with the 5Nb2.5P-500 samples after reusing in two or three catalytic cycles in the two different solvents (vide infra).

The survey spectra (Fig. S3) of the dried and calcined gels only shows the presence of the main elements constituting the material (Si, Nb, O and P) together with small amounts of carbon as a surface contaminant or also as a residue of the synthesis, in the dried sample. The composition of the samples calculated using the peak areas is reported in Table 4. It is possible to observe that the experimental Nb:P ratio well agrees with the expected stoichiometry. The main difference in the composition is observed in the carbon content, which is lower in the calcined sample than in the dried one.

Binding energy values of the main photoelectron peaks for the analyzed 5Nb2.5P samples are listed in Table 5. C 1s signal consists of three peaks in both dried gel and calcined samples. The most intense component is found at 285.0 (0.1) eV and it is assigned to aliphatic carbon. The component at 286.5 (0.1) eV is due to the presence of carbon in C-OH and the one at about 288 eV is ascribed to $R_2C{=}O$ [20]. Nb 3d signal consists of a spin – orbit doublet; the energy separation Nb $3d_{3/2}$ – Nb $3d_{5/2}$ is 2.7 eV and the area ratio of the two components is 2:3. Nb 3d is found at 208.5 (0.1) eV and it is ascribed to Nb^{+5} involved in Si–O–Nb–O bonds [21] since the binding energy of Nb $3d_{5/2}$ in bulk Nb_2O_5 is expected to be 207.5 eV, thus confirming the presence of Nb–O–Si bridges, also suggested by NMR analysis. [22]. Si 2p peaks were found at 103.6 (0.1) eV in agreement with the results reported by [22] for Nb_2O_5/SiO_2 mixed oxides. O1s was fitted with three components for the dried gel, being the components located at 530.9 (0.1) eV and 533.0 (0.1) eV related to oxygen involved in Nb–O bonds and in SiO_2 respectively [22]. The intense component at 533.8 eV, which might be due to adsorbed water, is not observed in 5Nb2.5P-500.

As far as the P signal, it is detected before and after calcination. The doublet P $2p_{3/2}$ – P $2p_{1/2}$ was separated by 0.9 eV, the binding energy of the P $2p_{3/2}$ was found to be 134.2 (0.1) eV and it is in pretty good agreement with phosphorus in ortophosphate moieties in phosphate glasses [23] and with the results reported by [21] for SiO_2/Nb_2O_5 mixed oxides surface modified by phosphoric acid.

These data confirm the existence of P–OH groups on the surface of both dried and calcined materials.

It is interesting to observe that the O:Nb ratio calculated for 5Nb2.5P-500 considering only the O1s component at 531.0 eV is found to be 2.4, which is in very good agreement with the Nb_2O_5 stoichiometry, and the O:Si ratio taking into account only the component at 533.0 eV is 1.9. For 5Nb2.5P dried gel, the O:Nb and O:Si ratios were found to be 2.7 and 1.7 respectively.

As concerns the reused catalysts after the II run in water and after the III run in water-isopropanol solution, a remarkable increase of the C/Si atomic ratio occurs, going from about 0.35 in the fresh catalyst (5Nb2.5P-500) to about 3.2 and 1.7 in the reused samples in water and water-isopropanol mixture, respectively (Table 4). This indicates that carbonaceous by-products of the reaction might coat the surface of both reused catalysts. The presence of this carbonaceous layer alters the atomic ratios of the other catalyst components giving a Si/Nb atomic ratio halved with respect to the fresh catalyst. The disappearance of the P signal can be explained as due to both its partial leaching and attenuation by the carbonaceous layer (Fig. S4).

Nb 3d (Fig. S5) and Si 2p (Fig. S6) binding energies do not show any significant difference after the catalytic runs. C 1s peak shows the presence of aromatic carbon at 284.7 (0.1) eV (Fig. 4), an intense component due to carbon in alcohols or in ethers at 286.3 (0.1) eV and the component due to carbonyl group at 288.5 (0.1) eV. The aliphatic component at 285.0 (0.1 eV) is the least intense one [20]. In O 1s signal, together with the contributions due to the Nb-O and Si-O bonds, a peak due to water is observed. Oxygen in C-OH might be included in the signal assigned to SiO_2.

3.4 Catalytic conversion of fructose

The reaction of dehydration of fructose over solid acidic catalysts in water and polar-protic solutions is known to be a complex reaction with parallel, consecutive, and equilibrium steps with formation of many products [7, 8, 24]. The analytical method above reported (i.e., HPLC with a Sugar- Pack I column) is an easy and useful method for a quantitative analysis of fructose and

HMF, the most important formed product. However, other products are known to form, such as condensation products of fructose, as di-D-fructose dianhydrides (like, β-D-fructofuranose β-D-fructopyranose 2,1':3,2'-dianydride [9,25]) and the so-called *humins*. In the present paper, the discussion of the catalytic results has been focused on total conversion of fructose and selectivity to HMF over the two gel-derived 2.5NbP-500 and 5Nb2.5P-500 materials. Fig. 5 shows the trends of fructose conversion as a function of time at 130°C on the two catalysts in the two reaction solvents (water and water-isopropanol); repeated runs are shown, they can be considered to represent recycling tests of the catalytic activity. On the two fresh catalysts (I run) in water (Fig. 5, top), the reaction proceeded with regular increasing trends of conversion (typical of a global first order reaction [9]) with a low kinetics without any clear difference between the two catalysts. After 3000 min, fructose conversion did not reach 50% conversion and reaction rate had highly decreased. Likely, deactivation of surfaces occurred gradually with time, due to the deposition of *humins* and other by-products highly insoluble in water. In fact, used catalysts analysed by XPS showed a series of different families of *C-species* indicating the complexity of the formed by-products.

Unexpectedly during the II run, performed on the used catalyst after its washing, fructose was converted with higher rate than in the I run on both samples. Almost 40% conversion was observed after 1000 min of reaction on 2.5NbP-500 and after 500 min on 5Nb2.5P-500. Unfortunately, the higher reaction rate of the II run gave rise to the formation of many insoluble by-products, besides HMF, which deposited on the catalyst surfaces so limiting the possibility of recirculation of the solution at the desired rate (the catalysts created high back pressure in the catalytic tubular reactor). Therefore, the test was stopped before the attainment of 50% conversion. A different behaviour has been observed in water-isopropanol solution (Fig. 5, bottom). The trend and values of fructose conversion on 2.5NbP-500 fresh catalyst (I run) were similar to those observed in water but the reaction rate appeared higher, while much lower conversion was observed on 5Nb2.5P-500 and also in this case, the reaction rate seemed to increase with time. In water-isopropanol, two subsequent reaction runs (II and III) have been performed on both used catalysts washed with the solvent,

obtaining almost similar, or even better, linear conversions with respect to the I run. This behaviour indicated a good stability of the surfaces; the reaction by-products had higher solubility in the alcoholic solution and therefore the catalyst surfaces could remain cleaner than in water. XPS results seem to substantiate this hypothesis, being carbon amount in the samples used in water higher than in those used in water-isopropanol mixture (Table 4). It was sufficient to wash the catalysts to make them free from some C-deposits and to allow them to start working again. Also in this case, it was observed, in particular on 5Nb2.5P-500, the unexpected behaviour already described above for the reaction carried out in water, i.e. the catalysts seemed to be activated over time (conversion trend: I run < II run ~ III run). In order to put forward a justification for this behaviour, likely the hydrolytic effect of hot water (130°C) has to be considered. The surface X–O(H)–Y linkages, with X, Y = P and Nb, might be opened and new acid sites (P-OH and Nb-OH groups) might form, so justifying the improvement of activity in the fructose conversion with reaction time. This behaviour is more pronounced on 5Nb2.5P-500 because its surface initially presents a lower amount of Brønsted sites than 2.5NbP-500, as observed by PEA titration in cyclohexane (*intrinsic* acidity).

Concerning reaction selectivity, besides the desired HMF, which constitutes a final stable product of fructose conversion on our catalysts, some other species formed have been detected, such as four fructose dimers with increasing elution time in the chromatographic analysis (β-D-fruf β-D-fruf 2,1':3,2'; α-D-fruf β-D-fruf 1,2':2,1'; α-D-fruf β-D-frup 1,2':2,1'; β-D-fruf β-D-frup 1,2':2,1'). Moreover, the formation of a heavier soluble condensation product (CP1) was observed, likely an oligomer of HMF, as our first analytical evidence seems to indicate. CP1 was observed in the HPLC chromatogram at the lowest retention time, typically the zone in which soluble oligosaccharides are observed. However, as CP1 was extracted from the solution containing the reaction products with methylisobutyl ketone (MIBK), it should be associated to a compound different from oligosaccharides. CP1 was formed in high amount with a yield even higher than HMF. Studies are in progress to recognize this species.

Selectivity to HMF in water-isopropanol attained 45% in the I run on 2.5NbP-500 and lowered to ca 30% in the II and III runs while lower selectivity to HMF has been observed on 5Nb2.5P-500 (up to 30%). A comparative view of catalytic performances in fructose dehydration reaction on the two Nb-P-Si catalysts during the three activity runs as observed at definite reaction time is displayed in Fig. 6. It emerges the quite satisfactory stability of 2.5NbP-500 in terms of conversion and HMF selectivity and the improved catalytic activity of 5Nb-2.5P-500 in the II run, while on the latter, a loss of HMF selectivity accompanied the III activity run.

4. Conclusions

Nb-P-Si mixed oxide catalysts are interesting solid acids that can be used with good performances in important reactions of sugar valorisation, as fructose dehydration. In particular, MAS-NMR characterization confirms that phosphorus is firmly anchored into the siloxane matrix of 5Nb2.5P catalyst. The homogenous composition of the surfaces of the materials has been also confirmed by XPS.

Both the Nb-P-Si oxide catalysts maintained lively acidity in polar-protic environments (water and water-isopropanol) responsible of their good activity in the fructose dehydration reaction. In water the reaction rate remarkably increased in the second run, likely owing to the partial hydrolysis of oxygen bridging bonds. On the other hand, in water-isopropanol solution the catalytic activity had higher stability than in water because in the former reaction environment a lower deposition of *humins* on the catalyst surface occurred.

The results obtained show that in order to obtain active and durable catalysts for the reactions of sugar valorisation, which are known to be strongly limited by deactivation caused by by-products, materials with suitable acid characteristics as well as proper solvents have to be chosen.

The promising catalytic activity observed on Nb-P-Si oxides is worthy of further investigation.

Acknowledgments

Dr. Maria Manuela Errico (Institute of Polymers, Composites and Biomaterials, IPCB-CNR, Pozzuoli, Naples) is acknowledged for solid state NMR measurements. The authors of the University of Milano gratefully thank Dr. Giovanni Paganoni past-student of University of Milano for the experimental support. This work was undertaken with financial support from the University of Cagliari and the Italian Ministry of the Education and University (MIUR). A. Rossi thanks Fondazione Banco di Sardegna and Regione Autonoma della Sardegna Progetti Biennali di Ateneo Annualità 2016, Fondazione Sardegna CUP F72F16003070002 for the financial support.

Supplementary data associated with this article can be found, in the online version, at the address: http://dx.doi.org/10.1016/j.apcata.xxxxxxxxxx.

REFERENCES

(1) P. Sudarsanam, R. Zhong, S. Van den Bosch, S. M. Coman, V. I. Parvulescu, B. F. Sels, Chem. Soc. Rev. 47 (2018) 8349-8402.

(2) N. J. Clayden, G. Accardo, P. Mazzei, A. Piccolo, P. Pernice, A. Vergara, C. Ferone, A. Aronne, J. Mater. Chem. A 3 (2015) 15986-15995.

(3) A. Aronne, M. Di Serio, R. Vitiello, N. J. Clayden, L. Minieri, C. Imparato, A. Piccolo, P. Pernice, P. Carniti, A. Gervasini, J. Phys. Chem. C 121 (2017) 17378-17389.

(4) A. Gervasini, P. Carniti, F. Bossola, C. Imparato, N. J. Clayden, P. Pernice, A. Aronne, Mol. Catal. 458 (2018) 280-286.

(5) R.-J. Van Putten, J. C. Van der Waal, E. De Jong, C. B. Rasrendra, H. J. Heeres, J. G. De Vries, Chem. Rev. 113 (2013) 1499-1597.

(6) T. M. László, E. Cséfalvay, Á. Németh, Catalytic Conversion of Carbohydrates to Initial Platform Chemicals, Chem Rev. 118 (2018) 505-613.

(7) C. Carlini, M. Giuttari, A. M. Raspolli Galletti, G. Sbrana, T. Armaroli, G. Busca, Appl. Catal. A 183 (1999) 295.

(8) T. Armaroli, G. Busca, C. Carlini, M. Giuttari, A. M. Raspolli Galletti, G. Sbrana, J. Mol. Catal. A 151 (2000) 233.

(9) P. Carniti, A. Gervasini, S. Biella, A. Auroux, Catal. Today 118 (2006) 373.

(10) S. K. R. Patil and C. R. F. Lund, Energy Fuel, 25 (2011) 4745-4755.

(11) I. van Zandvoort, Y. Wang, C. B. Rasrendra, E. R. H. van Eck, P. C. A. Bruijnincx, H. J. Heeres, and B. M. Weckhuysen, ChemSusChem 6 (2013) 1745-1758.

(12) P. Carniti, A. Gervasini, M. Marzo, Catal. Today 152 (2010) 42-47.

(13) P. Carniti, A. Gervasini, Liquid-solid adsorption properties: Measurement of the effective surface acidity of solid catalysts. Calorimetry and Thermal Methods in Catalysis. A. Auroux (Ed.), 2013, 17, Springer Series in Materials Science, 154.

(14) P. Carniti, A. Gervasini, F. Bossola, V. Dal Santo, Appl. Catal. B: Environ. 193 (2016) 93-102.

(15) M. Marzo, A. Gervasini, P. Carniti, Carbohydr. Res. 347 (2012) 23-31.

(16) T. Okuhara, Chem. Rev. 102 (2002) 3641-3666.

(17) I. Nowak, M. Ziolek, Chem. Rev. 99 (1999) 3603-3624

(18) J. C. Védrine, Res. Chem. Intermed. 41 (2015) 9387-9423.

(19) P. Carniti, A. Gervasini, S. Biella, A. Auroux, Chem. Mater. 17 (2005) 6128-6136.

(20) D.Atzei, M. Fantauzzi, A. Rossi, P. Fermo, A. Piazzalunga, G.Valli, R. Vecchi, Appl. Surf. Sci. 307 (2014) 120-128.

(21) M. S. P. Francisco, W. S. Cardoso, Y. Gushikem, R. Landers, Y. V. Kholin, Langmuir, 20 (2004) 8707-8714.

(22) M. S. P. Francisco, R. Landers, Y. Gushikem, J. Solid State Chem. 177 (2004) 2432-2439.

(23) M. Crobu, A. Rossi, F. Mangolini and N. D. Spencer, Anal. Bioanal. Chem. 403 (2012) 1415-1432.

(24) C. Moreau, R. Durand, S. Razigade, J. Duhamet, P. Faugeras, P. Rivalier, P. Ros, G. Avignon, Appl. Catal. A 145 (1996) 211-224.

(25) J. Defaye, A. Gadelle, C. Pedersen, Carbohydr. Res. 136 (1985) 53-65.

Table 1. Chemical shifts, δ (ppm), estimated relative intensities, I, and full width at half maximum, Fw (ppm), calculated from line fitting of the ^{29}Si resonances. For δ, I and Fw standard errors for are: ±0.25 ppm, ±0.01 and ±0.5, respectively.

	δ	I	Fw
5Nb2.5P	-91.2	0.08	3.4
	-100.2	0.36	2.9
	-109.5	0.56	3.5
5Nb2.5P-500	-92.3	0.12	4.5
	-100.10	0.30	2.9
	-109.18	0.58	4.0
5Nb2.5P-500-w	-91.7	0.09	3.8
	-100.10	0.33	3.1
	-108.99	0.58	3.9
2.5NbP-500	-91.2	0.07	3.9
	-101.4	0.31	2.9
	-110.3	0.62	3.9

Resonance assignments: -90.0 to -95.0 ppm: Q_2 $Si(OSi)_2(OH)_2$; -100.0 to -103.0 ppm: Q_3 $Si(OSi)_3(OH)$ and Q_2 $Si(OSi)(OH)_2(OX)$ with X = Nb, P; -109.0 to -112.0 ppm: Q_4 $Si(OSi)_4$ and Q_3 $Si(OSi)_2(OX)(OH)$ with X. Nb, P; -112.0 to -120.0 ppm: Q_4 $Si(OSi)_{4-x}(OP)_x$ with x = 1-3.

Table 2. Chemical shifts, δ (ppm), estimated relative intensities, I, and full width at half maximum, Fw (ppm), calculated from line fitting of the ^{31}P resonances. For δ, I and Fw standard errors for are: ±0.25 ppm, ±0.01 and ±0.5, respectively.

	δ	I	Fw
5Nb2.5P	-0.6	0.05	1.0
	-4.3	0.42	4.0
	-7.4	0.52	5.8
5Nb2.5P-500	-5.3	0.33	4.9
	-12.0	0.43	6.2
	-19.9	0.24	8.7
5Nb2.5P-500-w	-5.2	0.35	4.9
	-12.0	0.39	5.6
	-19.9	0.25	7.6

Resonance assignments: around 0 ppm: Q'_0 $OP(OH)_3$; -1.7 to -8.9 ppm: Q'_1 $OP(OX)(OH)_2$ with X = P, Nb; -10.5 to -22.5 ppm: Q'_2 $OP(OX)_2(OH)$ with X = P, Nb.

Table 3. Morphological and acidic properties of the two studied catalysts: total and microporous specific surface area ($m^2\ g^{-1}$), mesopore volume ($cm^3\ g^{-1}$, determined by BJH model), micropore volume ($cm^3\ g^{-1}$, determined by t-plot); and total acid sites (mequiv·g^{-1}, determined by PEA adsorption in different solvents).

Sample	Total Specific Surface Area	Microporous Specific Surface Area	Mesoporous Pore Volume	Microporous Pore Volume	Total acid sites		
					Intrinsic Acidity	*Effective* Acidity	
					cyclohexane	H_2O	H_2O–i-PrOH (80/20 v/v)
2.5NbP-500	377	160	0.101	0.072	0.605±0.005	0.304±0.023	0.327±0.012
5Nb2.5P-500	322	153	0.018	0.068	0.189±0.020	0.173±0.006	0.141±0.005

Table 4. Quantitative composition of the studied 5Nb2.5P samples – Accuracy is estimated to be ± 10%.

	C	O	Si	Nb	P
5Nb2.5P dried gel	14	60	23	2	1
5Nb2.5P-500	9	62	26	2	1
5Nb2.5P-500 used H_2O	39	47	12	2	-
5Nb2.5P-500 used i-prOH	28	52	16	3	-

Table 5. Binding energy values of the main photoelectron lines (eV) of the analyzed 5Nb2.5P samples. The reported values were determined by curve fitting the original spectra using Gaussian-Lorentzian product functions following iterative Shirley-Sherwood background subtraction. The area percentage of C components is reported in parentheses. The uncertainty of the binding energy values is estimated to be ± 0.2 eV.

	5Nb2.5P	5Nb2.5P-500	5Nb2.5P-500 used H_2O	5Nb2.5P-500 used H_2O–i-PrOH
C1s I (aromatic)	--	--	284.7 (17%)	284.7 (20%)
C1s I (aliphatic)	285.0 (21%)	285.0 (60%)	285.0 (8%)	285.0 (15%)
C1s (III) (C-OH; C-O-C)	286.2 (60%)	286.2 (37%)	286.2 (54%)	286.3 (47%)
C1s (IV) (carbonyl)	288.5 (19%)	288.5 (2%)	288.5 (21%)	288.5 (19%)
O1s: Nb-O	530.9	530.9	530.9	530.9
O1s: SiO_2	532.8	533.0	533.0	532.9
O1s: water	533.8		534.0	534.0
Si 2p	103.7	103.7	103.7	103.7
Nb – O – Si	208.5	208.4	208.3	208.4
P-O	134.2 (0.1)	134.2 (0.1)	-	-

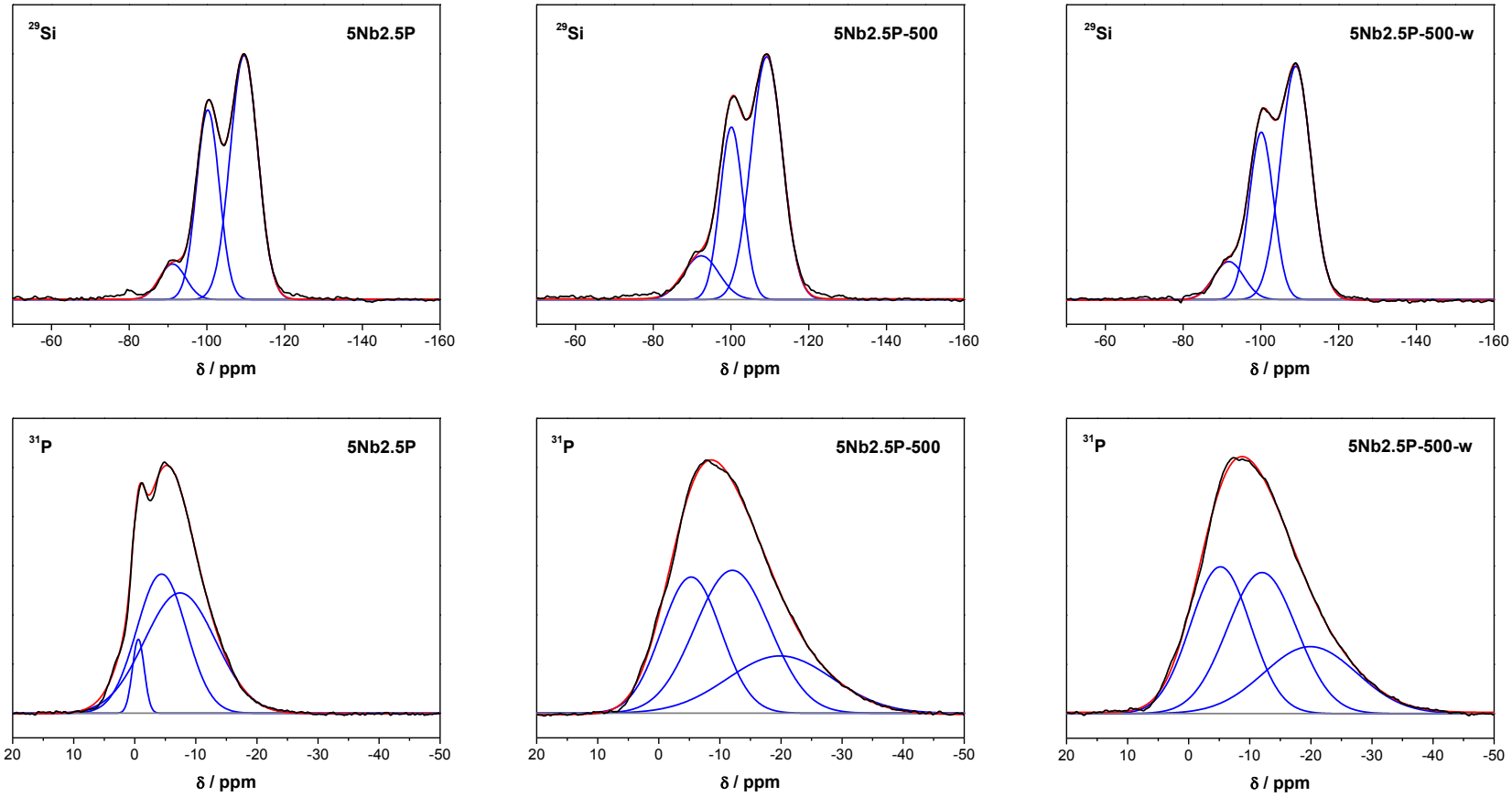

Fig. 1. ^{29}Si (top) and ^{31}P (bottom) MAS NMR spectra of the studied 5Nb2.5P samples. Black curve: experimental data; red curve: fitting curve; blue curves: fitting peaks.

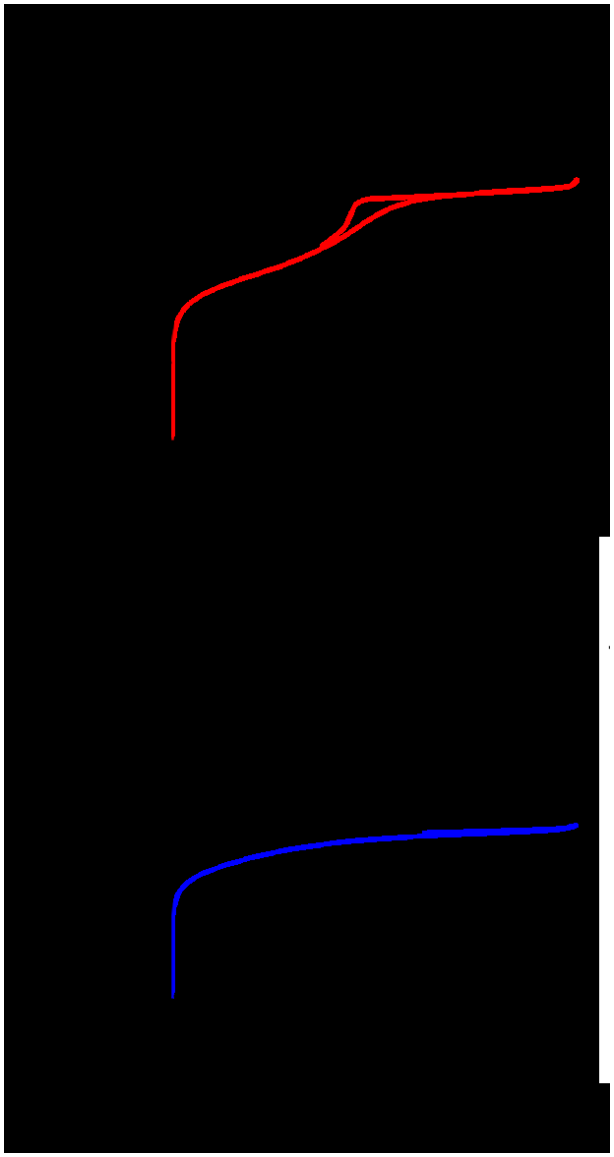

Fig. 2. N_2 adsorption/desorption isotherms at -196°C on 2.5NbP-500 (top) and 5Nb2.5P-500 (bottom). Pore size distributions relative to the samples are reported in Fig. S2.

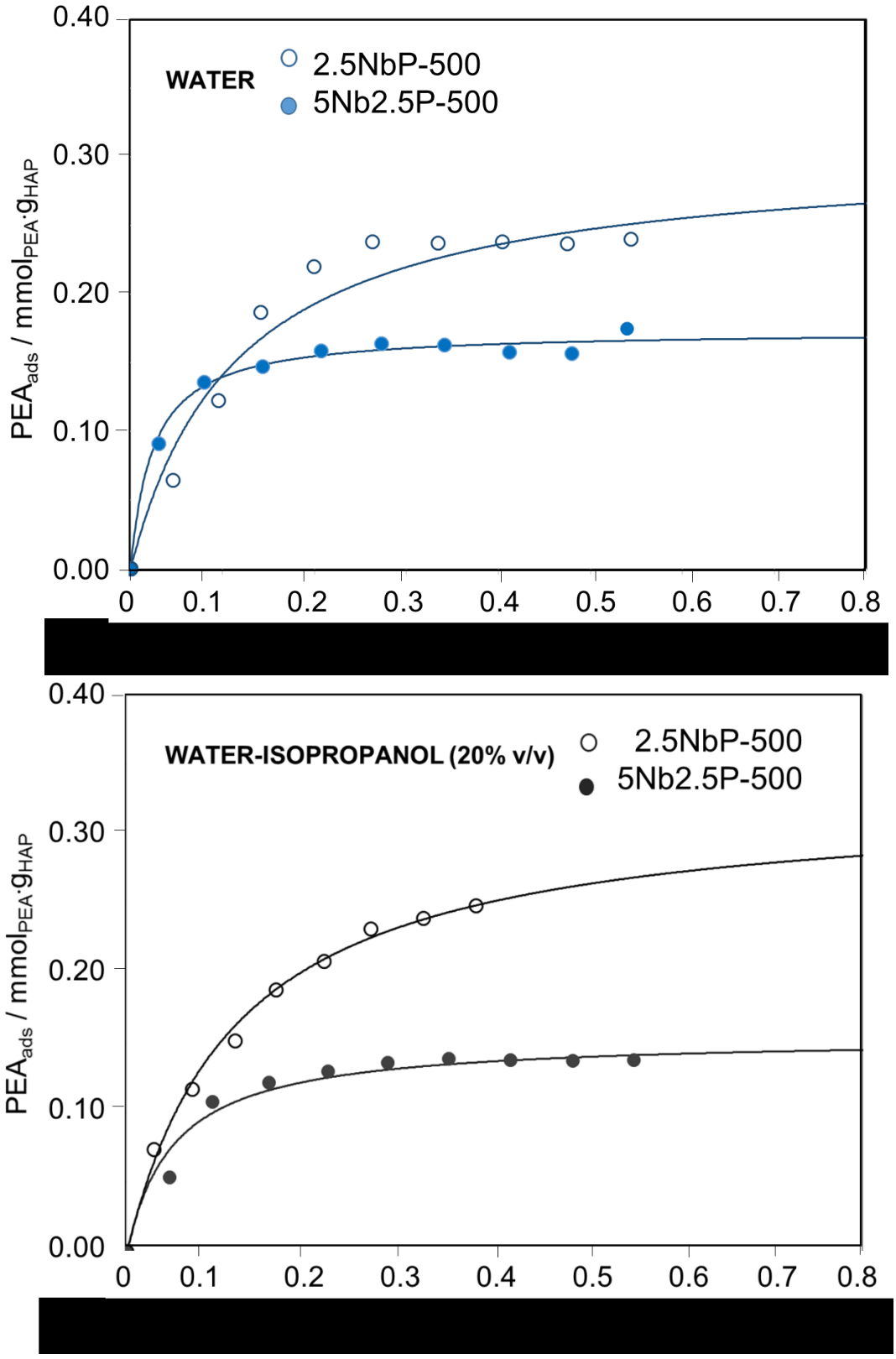

Fig. 3. Adsorption isotherms of PEA probe at 30°C on 2.5NbP-500 (empty markers) and 5Nb2.5P-500 (full markers) samples for determining the *effective* acidity in water (blue lines) and water-isopropanol solution (black lines). Solid lines represent the calculated Langmuir curves of PEA adsorption.

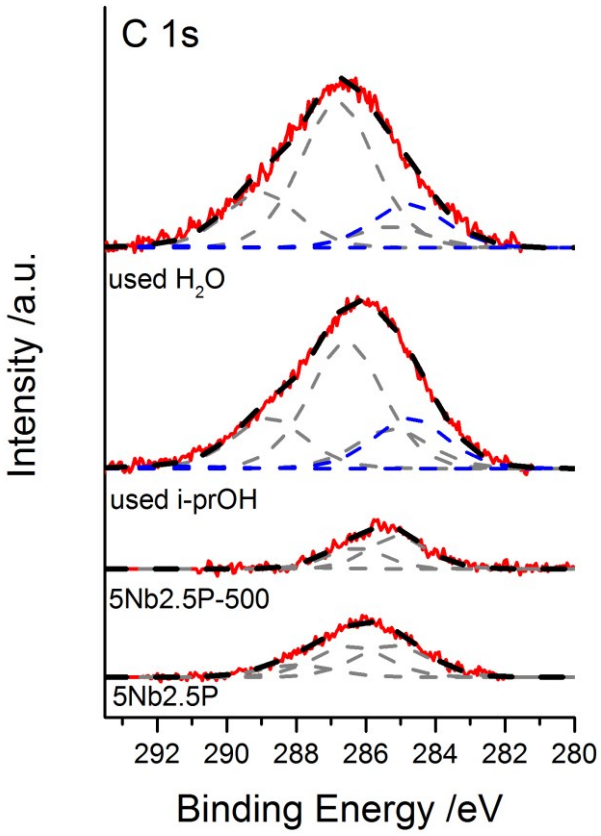

Fig. 4. XPS C1s spectra recorded on 5Nb2.5P dried gel, calcined and used samples.

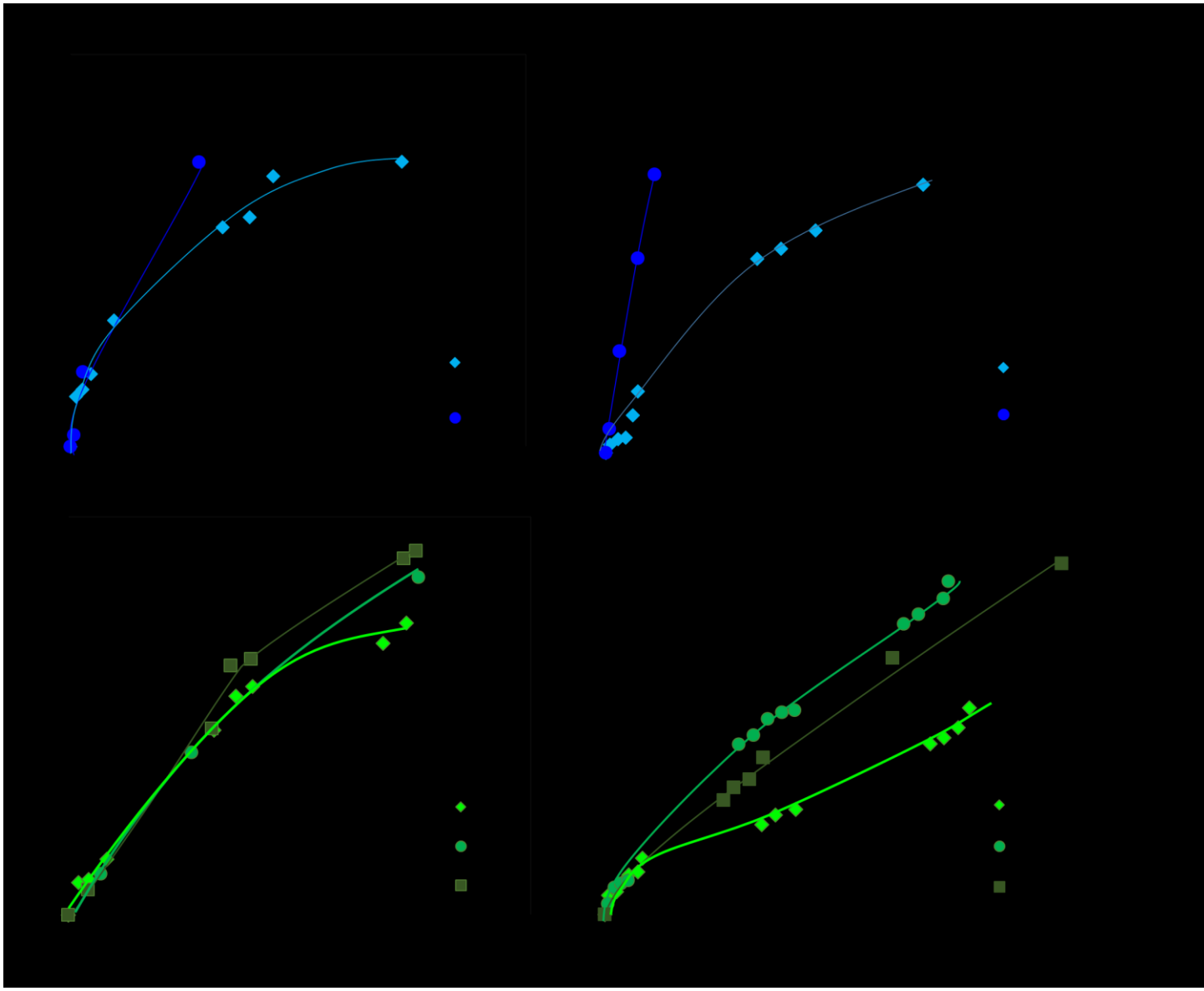

Fig. 5. Catalytic tests of fructose conversion on 2.5NbP-500 (left) and 5Nb2.5P-500 (right) catalysts as a function of reaction time; reaction has been carried out in a complete recirculation line with powder catalyst sample put in a flow tube reactor. First run on fresh catalyst, successive runs on used catalysts after washing with fresh solvent (water or water-isopropanol).

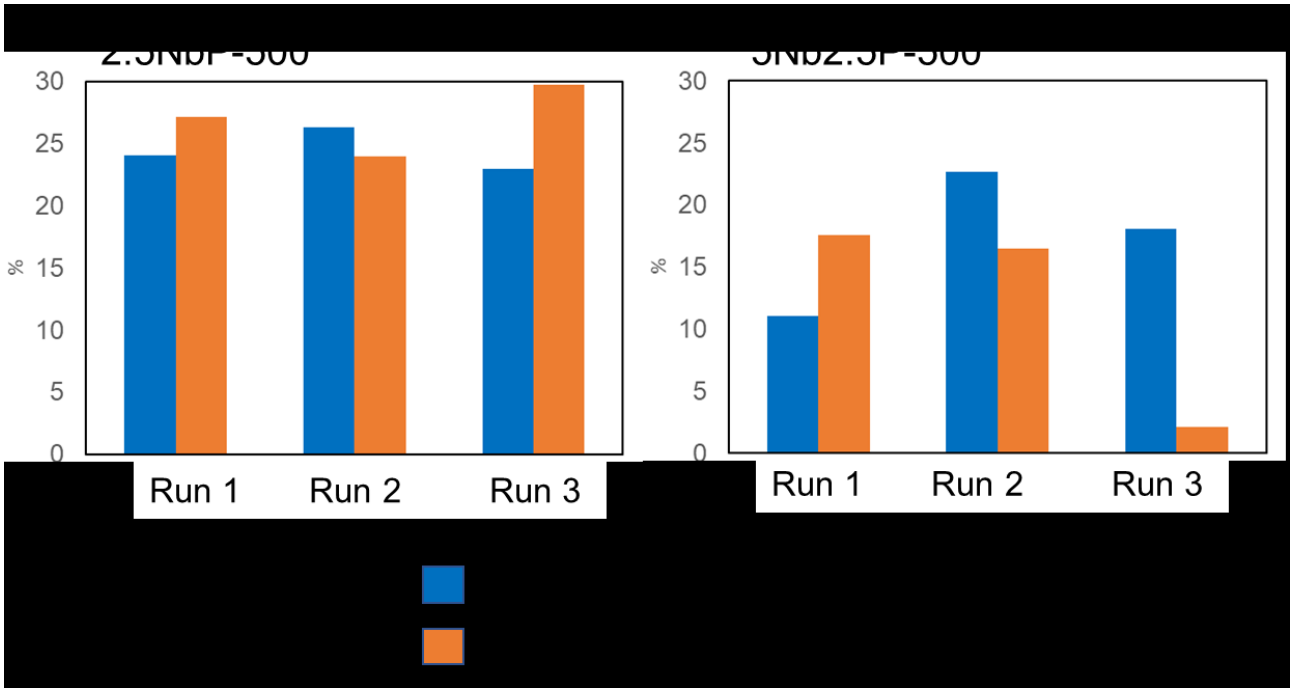

Fig. 6. Catalytic tests of fructose conversion on 2.5NbP-500 and 5Nb2.5P-500 catalysts in water-isopropanol solution: fructose conversion and selectivity to HMF after 1300 min on over three activity runs.

Supporting Information

Influence of Nb/P ratio of acidic Nb-P-Si oxides on surface and catalytic properties

S. Campisi,[a] P. Carniti,[a,b] A. Gervasini,[a,b,*] M. Fantauzzi,[c,d] C. Imparato,[f] N. J. Clayden,[e] A. Aronne [f,*] A. Rossi,[c,d]

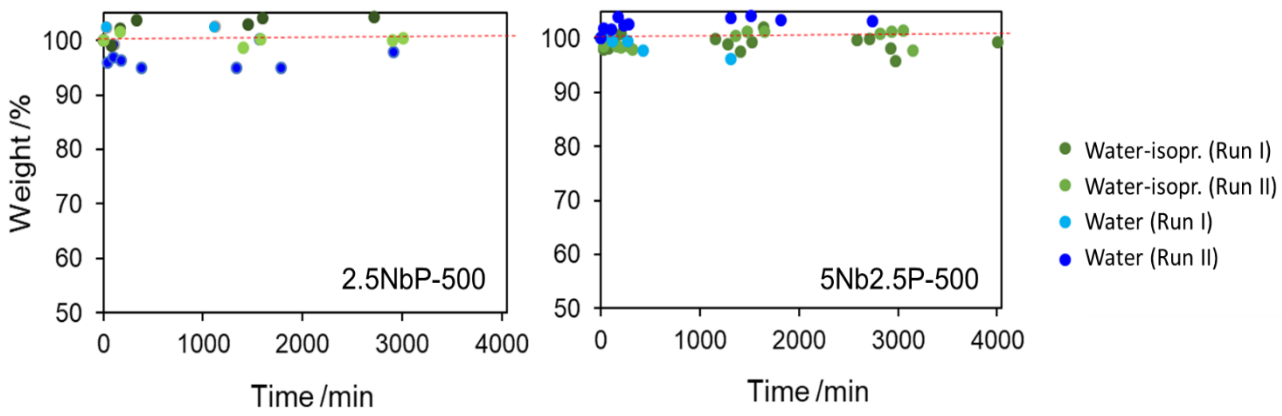

Fig. S1. Mass balance against time on 2.5NbP-500 and 5Nb2.5P-500 for all the catalytic tests.

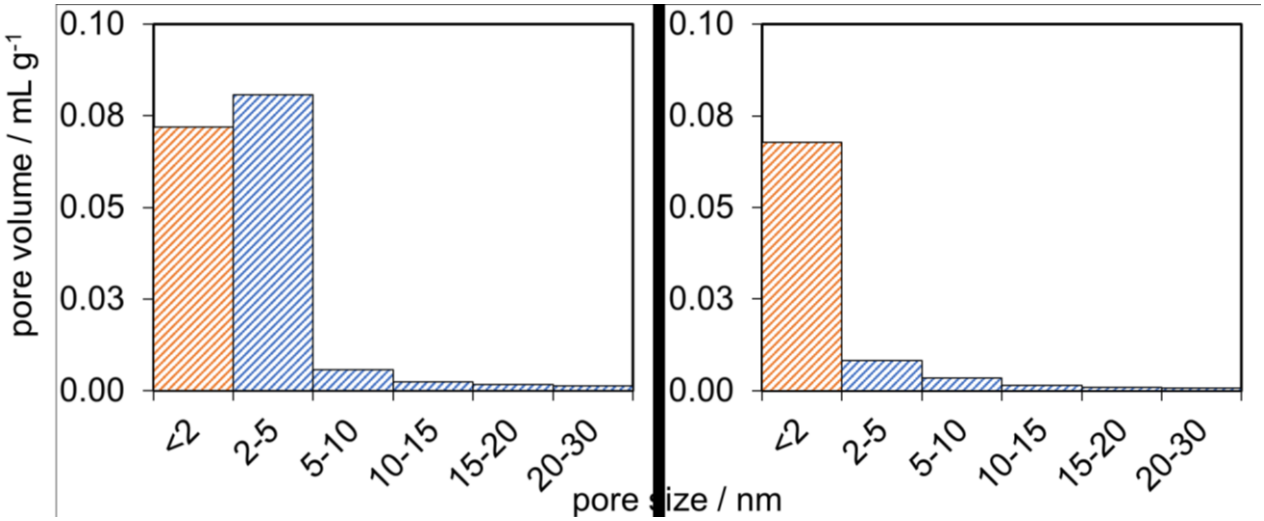

Figure S2. Pore size distribution of 2.5NbP-500 (left) and 5Nb2.5P-500 (right).

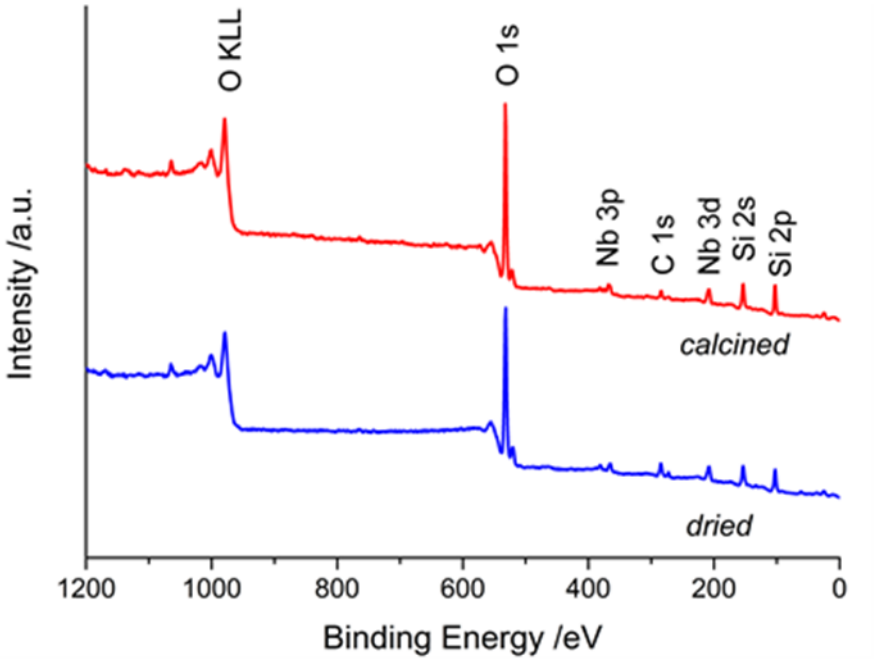

Fig. S3. Survey XP-spectra of dried 5Nb2.5P and calcined (5Nb2.5P-500) samples (X-ray source: Al Kα).

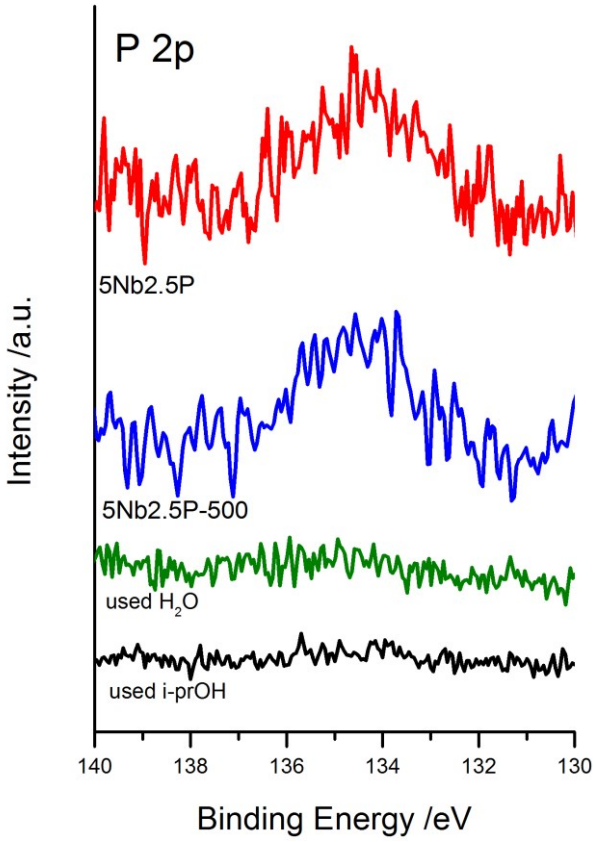

Fig. S4. P 2p XP-spectra recorded on 5Nb2.5P dried gel, calcined, and used samples.

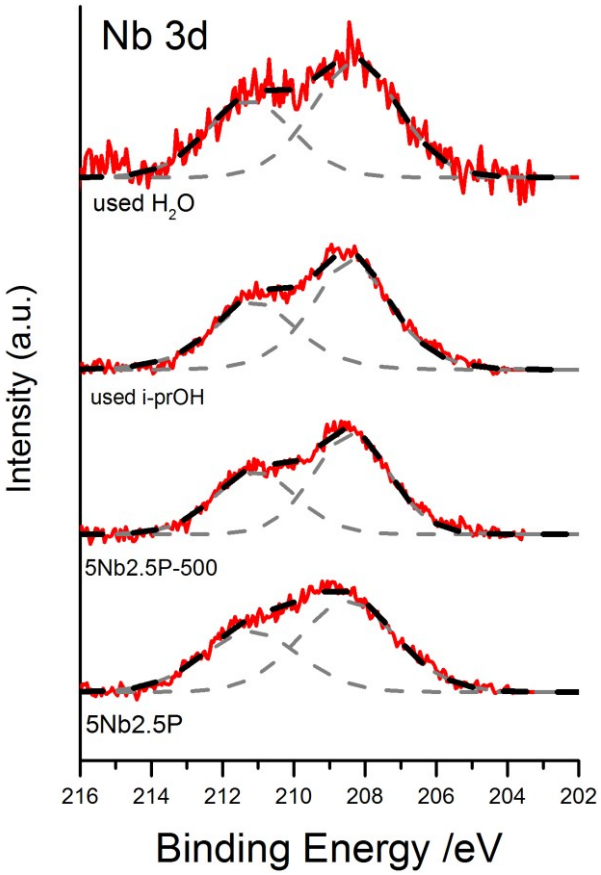

Fig. S5. Nb 3d XP-spectra recorded on 5Nb2.5P dried gel, calcined, and used samples.

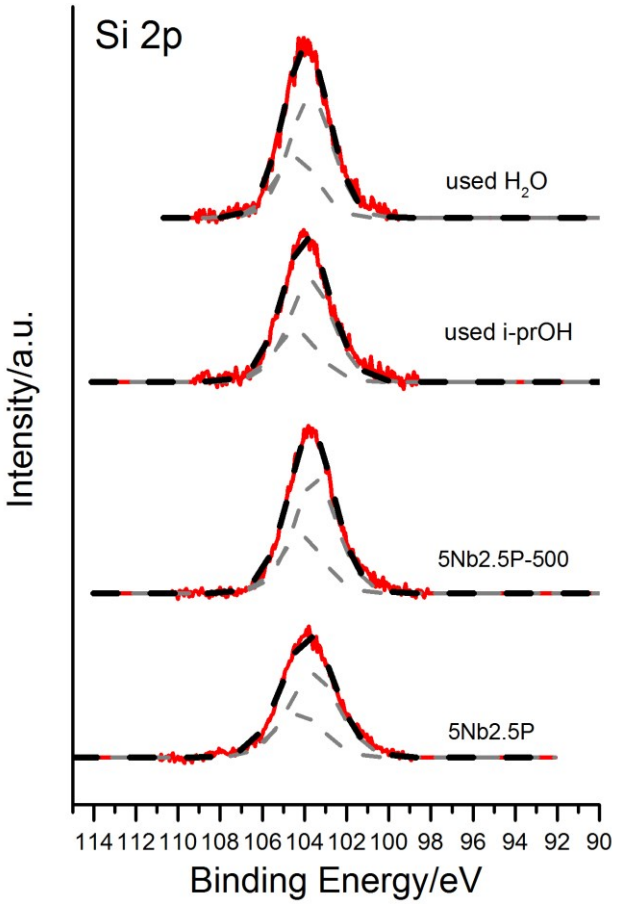

Fig. S6. Si 2p XP-spectra recorded on 5Nb2.5P dried gel, calcined, and used samples.

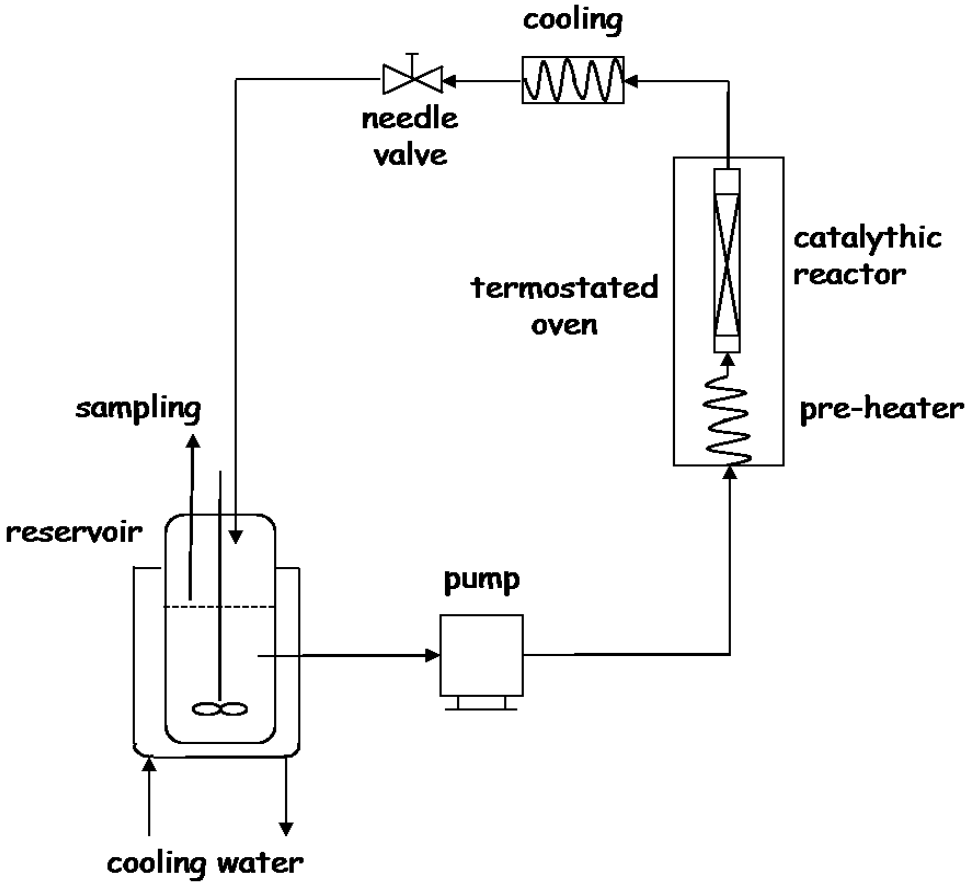

Scheme S1: Scheme of the reaction line used for the catalytic tests of fructose conversion in complete recirculation of solution; the catalytic reactor worked at 130°C under pressure.